Section I – Mass Loading and Supplemental Figures

The mass loading of particle stock suspensions was calculated using the dried masses of 0.250–4.000 mL of suspension. The mass of each weigh boat was recorded prior to the volumetric addition of the stock suspension and after the suspension dried at room temperature. Sample mass was determined by difference. Dried masses were plotted versus added volumes, where the slope defined the particle mass loading (Fig. S1).

Section II – X-ray Diffraction Calibration Curve Calculations and Figures

Calibration standards prepared with minerals of identical morphology, or nominally similar in the case of goethite, to ensure that the peak widths were comparable. Standards prepared in this way have been shown to be accurate to 1 mass% (Barron et al. 1997). While most of the calibration standards were prepared using rhombohedral hematite, two standards of 15 mass% and 30 mass% goethite were also made using equidimensional particles. With the size and morphology differences between the two hematite morphologies, the XRD patterns of pure particles showed a slight difference, namely that the particle size affected the peak width as seen in Figure S3. The equidimensional calibration standards, however, did not show a significant deviation from the linearity of the rhombohedral standards and thus the calibration curve was taken to be representative of both hematite morphologies.

To obtain reliable peak areas, one diffraction index from each mineral must be fully resolved from any nearby reflections and the selected diffraction index must be intensely scattering to maximize the signal to noise ratio. The goethite {110} and hematite {012} reflections are used here, shown in Figure S9.

As the goethite content increases, the {110} peak area is expected to increase. When graphing the goethite area fraction versus the goethite mass fraction, however, the trend is not linear because the scattering intensities of goethite and hematite differ. The area fractions were therefore adjusted for the scattering intensities to account for these differences. Generic calculations for this process are described in West (2014), and the detailed calculations for goethite {110} and hematite {012} are described below.

The atomic scattering amplitudes (f) for Fe and O were graphed versus *(sinθ)/λ* (Fig. S10), as tabulated in the International Tables for Crystallography, Volume C (Prince 2006), where θ is half the *2θ* peak position of the goethite {110} and hematite {012}, and λ is the Co K$_\alpha$ wavelength of the XRD X-ray source. Using known values of θ for goethite {110} and hematite {012} and λ based on the XRD analyses performed here, the atomic scattering amplitudes were found and are presented in Table S2.

Scattering intensity is proportional to the square of the diffracted sine waves, which can be transformed from complex notation and written as Equation S1. The phase difference (δ) (Equation S2) was calculated from the Miller indices and atomic positions of Fe and O, which are reported in Pauling and Hendricks (1925) for hematite and Szytula et al. (1968) for goethite (Table S3). For hematite, the hexagonal atomic positions were adjusted to Cartesian coordinates. For goethite, the (110) facet was reverted to the original labeling system (101) rather than adjusting the Fe and O atomic positions to correspond to the new labeling system. The current unit cell (abc) corresponds to (bca) when described by the original goethite space group Pbnm.

$$I_{hkl} \propto |F_{hkl}|^2 = \sum_j \left(f_j \cos \delta_j\right)^2 + \sum_j \left(f_j \sin \delta_j\right)^2 \tag{S1}$$

$$\delta = 2\pi(hx + ky + lz) \tag{S2}$$

By factoring in the scattering intensities using Equation S3 as the y-axis, the resulting linear calibration curve becomes a reliable tool for determining goethite mass percent (Fig. S11).

$$\frac{F_{Gt(110)}{}^2 Area_{Gt(110)}}{F_{Gt(110)}{}^2 Area_{Gt(110)} + F_{Ht(012)}{}^2 Area_{Ht(012)}} \tag{S3}$$
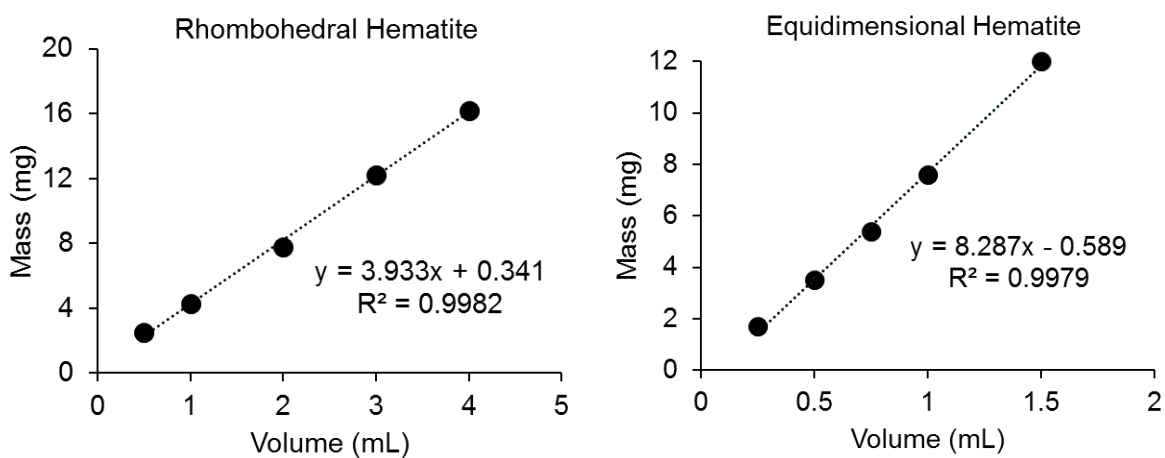
Figure S1. Mass loading plots for the stock suspensions of rhombohedral (left) and equidimensional (right) hematite. Slope of the fitted line describes mass loading in mg/mL of the suspension.
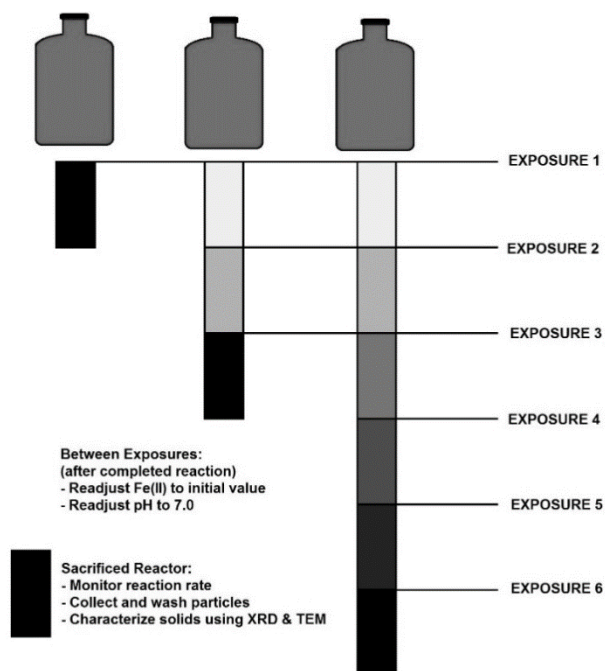
Figure S2. Reactor scheme for recurrent-exposure reactions. Single-exposure reactions are sacrificed after one exposure. Recurrent-exposure reactions are sacrificed after one, two, three, or six exposures of 4-ClNB. Between exposures, after the reaction is complete, the Fe(II) concentration is measured and readjusted to its initial value (Fig. S6), and then the pH is readjusted to 7.0. For a sacrificed reactor: the reaction rate is determined by HPLC sampling, the particles are collected and washed, and the solids are characterized by XRD and TEM to determine mineral composition and morphology.
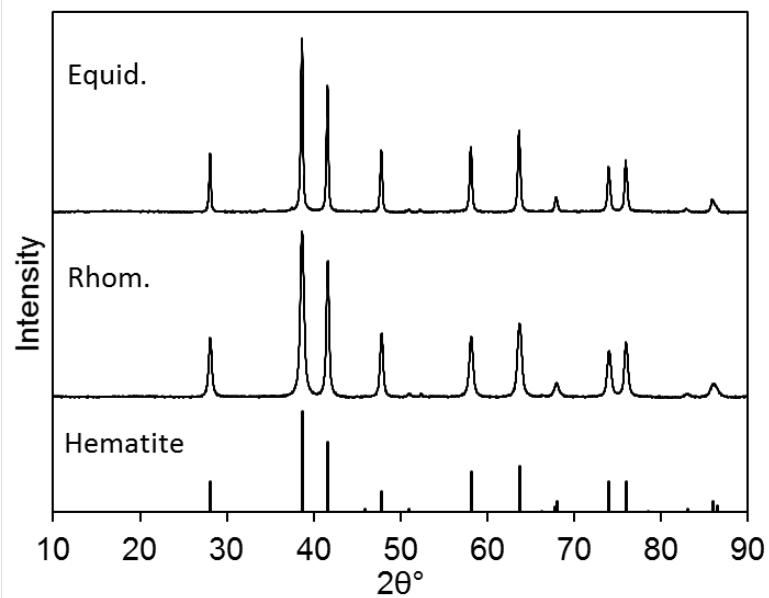
Figure S3. X-ray diffraction patterns of synthetic rhombohedral (R) and equidimensional (E)

hematite. Both are consistent with pure hematite, as compared to reference PDF 33-0664.
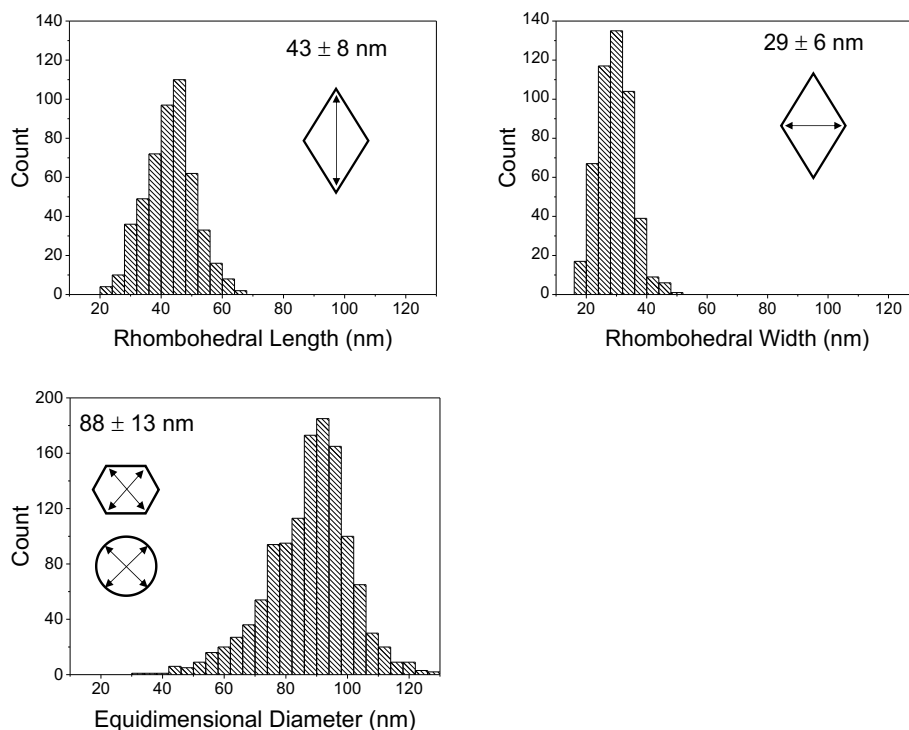
Figure S4. Measurement geometry for rhombohedral particles and equidimensional particles. Rhombohedral dimensions were calculated using 500 particles having clear boundaries in direction of measurement. Equidimensional measurements consisted of 500 particles, each having two perpendicular measurements. As some equidimensional particles exhibited an elongated hexagonal morphology, the measurements were made such that both perpendicular measurements represented the average size of the particle.
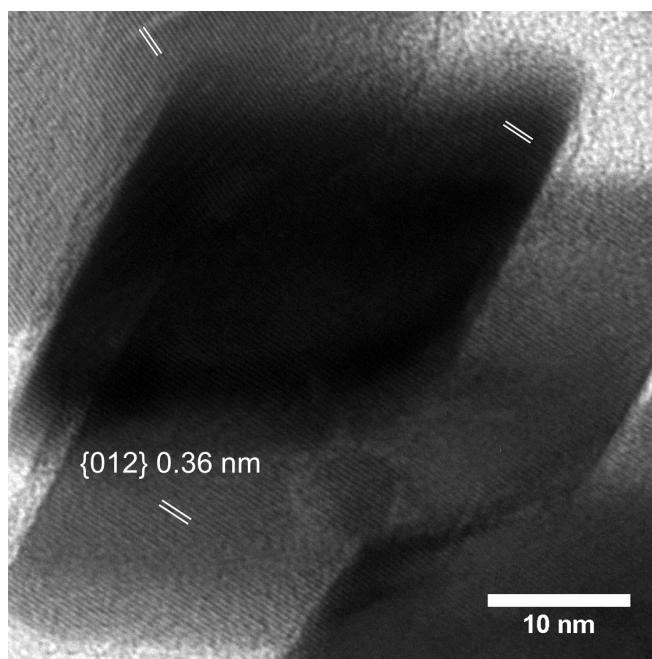
Figure S5. TEM image showing lattice fringes in pre-reaction rhombohedral (R) hematite. All white lattice indicators measure 0.36 nm, which corresponds to hematite {012}.
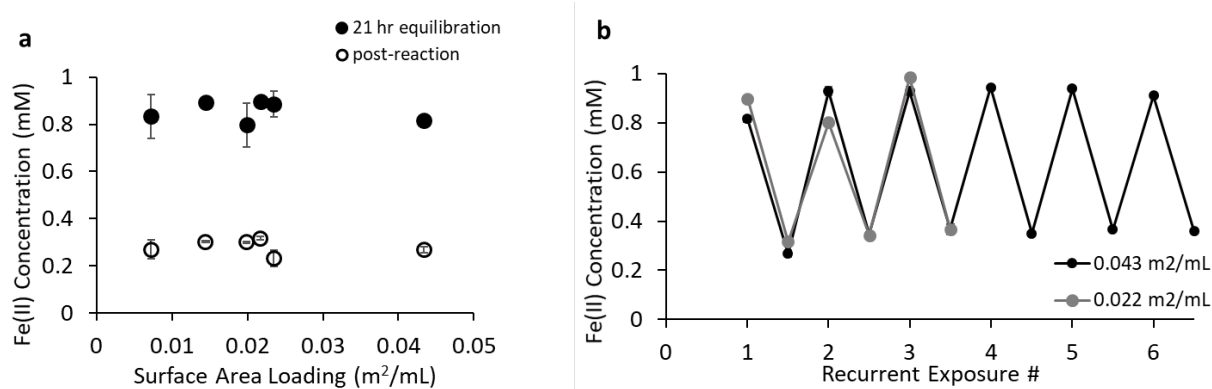

Figure S6. Iron(II) concentrations in (a) single-exposure reactors and (b) recurrent-exposure reactors after 21-hour equilibration and post-reaction. Error bars in both plots represent standard deviations. Data points are connected in recurrent-exposure reactors to guide the eye through changes in Fe(II) due to reaction and readjustment.
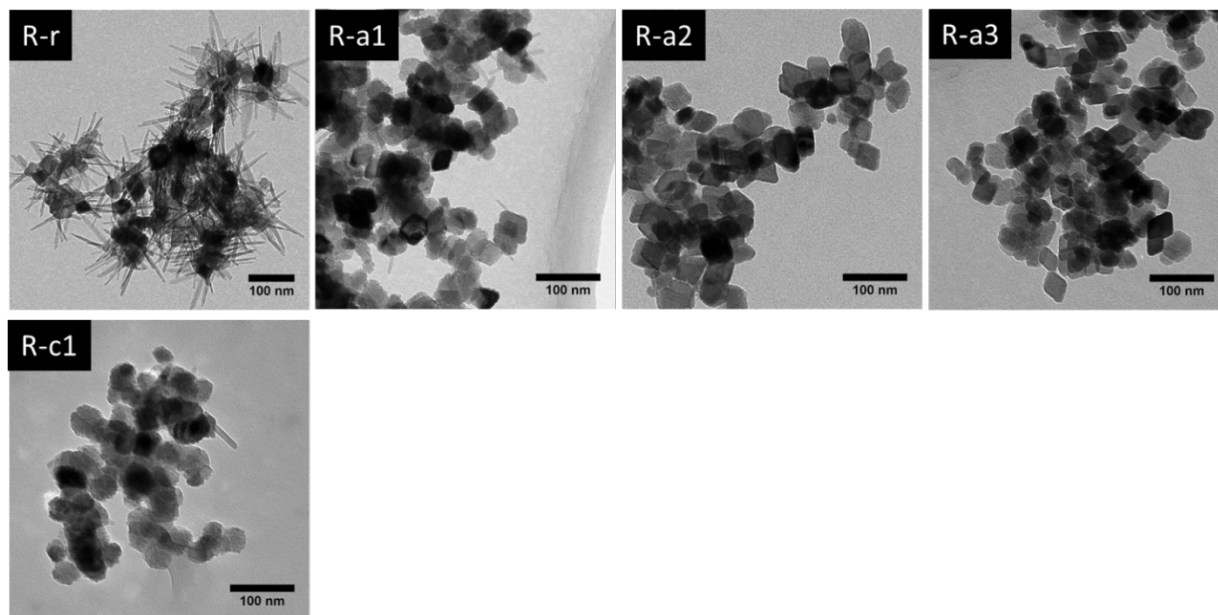
Figure S7. TEM images showing rhombohedral hematite particles after reaction with 100 uM 4-ClNB in the presence of 1 mM Fe(II) with increasing surface area loading (Table 1, Set a) and at pH 6.5 (Table 1, Set c) as compared to reference R-r. See Table 1 for sample identifiers.
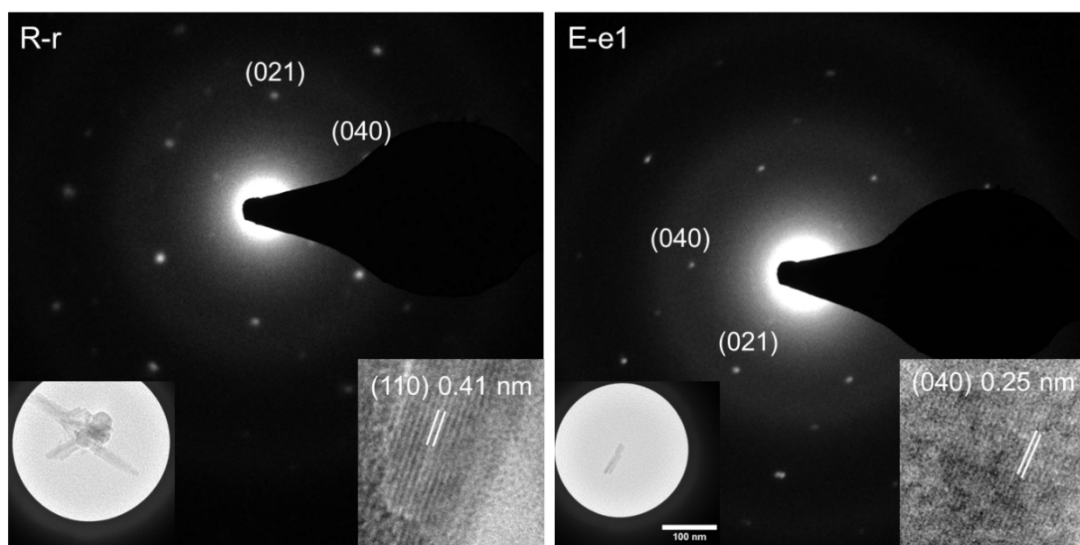

Figure S8. Additional TEM diffraction and lattice images showing the presence of goethite. Electron diffraction patterns are viewed down the [100] zone axis. See Table 1 for sample identifiers.
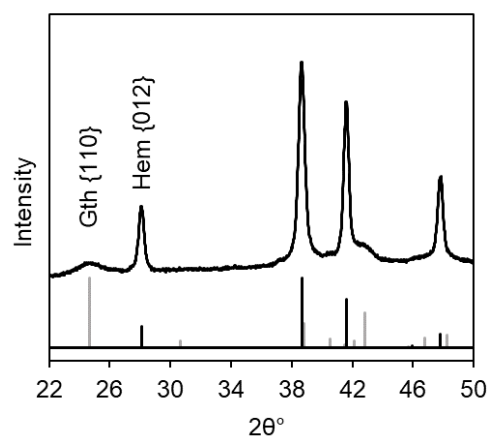
Figure S9. An unmodified x-ray diffraction pattern of reactor R-r showing the goethite {110} and hematite {012} reflections. The grey and black reference patterns are goethite and hematite, respectively.
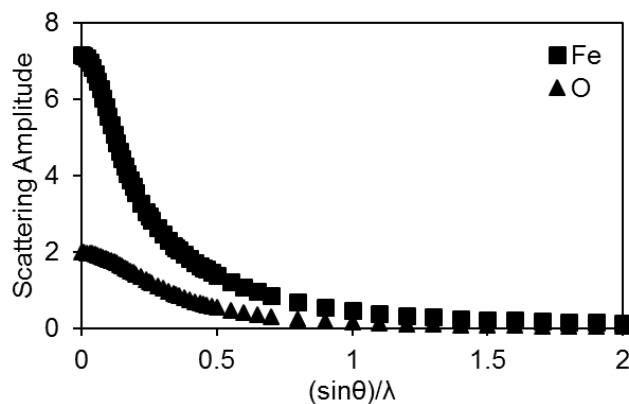
Figure S10. Atomic scattering amplitudes (f) for electrons of neutral atoms. Values for Fe and O are listed in International Tables for Crystallography, Volume C (Prince 2006).
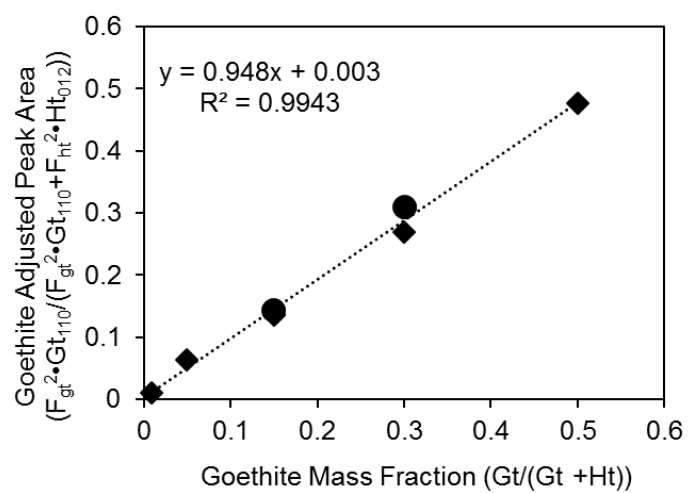
Figure S11. X-ray diffraction calibration curve showing goethite adjusted peak area versus goethite mass fraction for five rhombohedral hematite standards (diamonds) and two equidimensional standards (circle).

Table S1. Literature values for goethite reactivity.

Reference	Buffer	[4-ClNB] (μM)	[Fe(II)] (mM)	Volume (mL)	Mass Loading (mg/mL)	BET S.A. (m^2/g)	S.A. Loading (m^2/mL)	Reaction Rate (hr^{-1})
Vindedahl 2015	10 mM $NaHCO_3$	100	1.00	120	0.325	117	0.038	0.75
Stemig 2014	10 mM MOPS	100	1.00	50	0.325	117	0.038	0.90
Chun 2006	50 mM MOPS	100	1.00	123	0.650	137	0.089	3.42

Table S2. Constants and parameters involved in the calculation of scattering intensities of goethite and hematite.

	Constants	Hematite	Goethite
(hkl)		{012}	{110}
d-spacing (Å)		3.682	4.182
Co-K_α (Å)	1.7909		
θ °		14.075	12.364
(sin θ)/λ ($Å^{-1}$)		0.136	0.120
f_{Fe} (Å)		4.644	5.087
f_O (Å)		1.664	1.739
I_{hkl}		102.88	31.93

Table S3. Atomic positions of iron and oxygen in hematite and goethite reported in the literature (Pauling and Hendricks 1925; Szytula et al. 1968) adjusted to correspond to Cartesian coordinates in the case of hematite.

Hematite	x	y	z	Goethite[a]	x	y	z
Fe	0.105	0.105	0.105	Fe	0.145	0.250	-0.045
	-0.105	-0.105	-0.105				
	0.395	0.395	0.395				
	0.605	0.605	0.605				
O	0.292	-0.292	0.000	O	-0.199	0.250	0.288
	-0.292	0.000	0.292		-0.053	0.250	-0.198
	0.000	0.292	-0.292				
	0.208	0.792	0.500				
	0.792	0.500	0.208				
	0.500	0.208	0.792				

[a] The reported values are given according to the original goethite labeling system. For calculation purposes, the goethite (110) plane was translated into the original system (i.e. (101)) rather than translating the atomic coordinates to the current space group *Pbma*.